

Person-Based Adaptive Priority Signal Control with Connected-Vehicle Information

Xiaosi Zeng, Xin Sun, Yunlong Zhang, and Luca Quadrioglio

The goal for transit signal priority (TSP) strategies is to improve the efficiency of urban transportation systems by promoting fast passage of system users. However, because conventional vehicle detection technologies require TSP strategies to be vehicle based, TSP may not lead to optimal results for person delay. This paper proposes a signal control model called PAPSCCI (person-based adaptive signal priority control with connected-vehicle information). First, by using vehicle speed and location information available from connected-vehicle technologies, the model explicitly computes individual vehicle delay. In this way the model avoids assumptions about vehicle arrivals, which often are inevitable in a delay calculation derived from a queuing model. Furthermore, in the model approach, the computation of delays for private vehicles is no different from that for public buses except in the priority level and unifies the two types of vehicles. With onboard passenger information, the PAPSCCI model computes person delay for every vehicle running through the intersection and offers a more accurate basis for person delay minimization. The performance of the PAPSCCI model is evaluated in a traffic simulation environment. Compared with the optimized timing from SYNCHRO, the PAPSCCI model produces 39%, 49%, and 30% decreases in bus passenger delays for one, two, and three conflicting bus routes, respectively. In addition, general automobiles experience about an 8% to 11% decrease in person delays, showing the potential of PAPSCCI as a general adaptive signal control model. Finally, a penetration rate study shows that the PAPSCCI model can consistently perform reasonably well even when only about 30% of vehicles are equipped with connected-vehicle technology.

Public transit is key to relieving traffic congestion in densely populated cities. Transit signal priority (TSP) is an operational strategy that facilitates the movements of transit vehicles at signalized intersections. Since its implementation, many TSP strategies have been devised, including passive, active, and adaptive signal control (1, 2). Most commonly, green extension of the transit phase and red truncation of the nontransit phase are the main strategies for timing modification (1, 3–5).

Studies have found that attempting to assign signal priorities to transit vehicles inevitably causes negative impacts on the traffic operation of nontransit vehicles. Furthermore, when the number of conflicting buses increases, a first-come, first-serve TSP strategy may become inefficient. Because of these and other concerns, model-

based approaches have become more popular for accounting for many practical constraints simultaneously. Toward this goal, Ma et al. built an optimization model to minimize the bus delay by generating an optimal servicing sequence for multiple bus lines (6). Li et al. optimized green splits to minimize a weighted delay of both buses and other vehicles (7). Zeng et al. proposed a stochastic mixed-integer TSP model for explicitly modeling random bus arrival times (8). He et al. proposed a platoon-based formulation for optimizing arterial signal timings based on clustered signal requests with different priority levels (9).

The ultimate intention of providing signal priority to a vehicle of high passenger density is to help more persons through less delay. When vehicle-based TSP models could not fulfill that intention, person-based models were brought forward (10, 11). Christofa et al. showed that a person-based TSP model could achieve minimal overall person delay (10).

The detection system is a critical element in the design of an effective TSP strategy. By relying on separate detection channels from buses and autos, a TSP strategy must make assumptions about auto arrivals and must treat autos differently from buses. To estimate auto delays, deterministic queuing model is often used. More recently, connected-vehicle (CV) technology has served as an alternative detection system that provides enriched probe vehicle data to allow formulation of a TSP model with more details (12). Messages such as vehicle speed, location, acceleration rate, onboard passengers, and other information may be transmitted for use in building a less assumption-dependent model (13). Several studies have found greater performance of various transportation applications because of the use of CV technology (9, 14).

Under the CV paradigm, auto delays can be calculated individually, and overall auto delays can be aggregated additively. As a result, the computations of delays for private vehicles are no different from those for public buses, except they have a lower priority. By unifying the treatment of private and public vehicles for TSP modeling, this paper proposes a signal control model called PAPSCCI (person-based adaptive priority signal control with connected-vehicle information).

METHODOLOGY

The PAPSCCI model minimizes the total person delay of all vehicles at an intersection in mixed traffic. A few assumptions were made. First, the communication range of the CV technology at the intersection is assumed to be large enough to reach both autos and buses that will arrive within the planning horizon, which is set to be two cycles in this study. Second, the traveling speed, the number of passengers, and the requesting signal phase of a vehicle are assumed to be available from the CV technology.

X. Zeng, Traffic Technology Solutions, 17933 Northwest Evergreen Parkway, Beaverton, OR 97006. X. Sun, Y. Zhang, and L. Quadrioglio, Zachary Department of Civil Engineering, Texas A&M University, 3135 TAMU, College Station, TX 77843-3135. Corresponding author: X. Zeng, naoh.zeng@gmail.com.

Transportation Research Record: Journal of the Transportation Research Board, No. 2487, Transportation Research Board, Washington, D.C., 2015, pp. 78–87. DOI: 10.3141/2487-07

Objective Function

The PAPSCCI model treats every vehicle separately. The model minimizes the total person delay, which is the delay of all vehicles multiplied by their occupancy. For each optimization, all vehicles waiting at or waiting to arrive at the intersection within the planning horizon are included in this objective function.

$$\min Z = \sum_{j=1}^J \sum_{i=1}^{I_j^o} o_{i,j} d_{i,j}^o + \sum_{j=1}^J \sum_{i=I_j^o+1}^{I_j} o_{i,j} d_{i,j} \quad (1)$$

where

J = total number of phases running in this intersection,

I_j^o = number of vehicles that are waiting in the queue of phase j at the intersection when the optimization is carried out,

I_j = number of all vehicles that are approaching and will arrive at the intersection before the end of the planning horizon for phase j ,

$o_{i,j}$ = occupancy of the i th vehicle on phase j , and

$d_{i,j}^o, d_{i,j}$ = delay of the i th vehicle on phase j : $d_{i,j}^o$ applies to vehicles that are waiting in the queues when optimization is conducted, and $d_{i,j}$ refers to vehicles that are approaching the intersection.

The planning horizon is set as two cycles in this study. That is, when cycle k is being optimized, the delay of those vehicles approaching the intersection during cycle $k+1$ is also considered. In this way, the possible influences of each optimization on the following cycles are considered. Hence, the PAPSCCI model can ensure that each optimization will not leave accumulated negative impacts that could deteriorate the intersection's traffic operation in the future.

Optimization is conducted cycle by cycle. Each vehicle's free-flow travel time to the stop bar ($T_{i,j}^r$) is predicted by dividing the distance of the vehicle's current location from the stop bar by its current speed ($v_{i,j}$). All vehicles included in the optimization are given a unique index i , according to their arriving sequences or queuing position.

Modeling Standard Signal Behavior

For modeling the behavior of a standard ring-barrier-based signal control system, Head et al. proposed a simple yet effective precedence model (15). The PAPSCCI model adopts this concept to model the standard eight-phase, two-ring signal control logic in Equations 2 through 8:

$$t_{1,1} = t_{s,1} = 0 \quad (2)$$

$$t_{2,k} = t_{1,k} + v_{1,k}; t_{3,k} = t_{2,k} + v_{2,k}; t_{4,k} = t_{3,k} + v_{3,k} \quad (3)$$

$$t_{6,k} = t_{5,k} + v_{5,k}; t_{7,k} = t_{6,k} + v_{6,k}; t_{8,k} = t_{7,k} + v_{7,k} \quad (4)$$

$$t_{1,k+1} = t_{4,k} + v_{4,k}; t_{3,k+1} = t_{8,k} + v_{8,k} \quad (5)$$

$$t_{1,k} = t_{5,k}; t_{3,k} = t_{7,k} \quad (6)$$

$$t_{8,k+1} + v_{8,k+1} - t_{1,k} = 2C \quad (7)$$

$$v_{j,k} = g_{j,k} + Y + R \quad (8)$$

$$g_{j,k} \geq g_{\min,j} \quad (9)$$

where

$t_{j,k}$ = start time of green of phase j in cycle k ,

$v_{j,k}$ = phase split of phase j in cycle k ,

$g_{j,k}$ = green time of phase j in cycle k ,

C = background cycle length,

Y = yellow time, and

R = all-red time.

The first five constraints may be formulated differently for another phasing sequence. Constraint 7 sets the planning horizon to be exactly two cycle lengths, while the two cycles within the horizon could be of varying length. This setting means the signal controller could be more flexible in adjusting the timing within each cycle. Constraint 9 restricts the phase duration to having a lower bound.

Vehicle Delay

There are two delay types: (a) delay of vehicles that are already queuing at the intersection at the time of the optimization and (b) delay of those that will arrive within the planning horizon. The queuing delay is easy to calculate. For example, for the i th vehicle in the queue, the number of vehicles queuing ahead of it is $\lfloor (i-1)/N_j \rfloor$ (N_j is the number of lanes of phase j , and $\lfloor \cdot \rfloor$ is the flooring function). These vehicles will clear the intersection at the saturation flow rate (s_j) when the next green begins ($t_{j,k}$). Hence, its delay is calculated with Equation 10:

$$d_{i,j}^o \geq \frac{\lfloor (i-1)/N_j \rfloor}{s_j} + t_{j,k} - t_{i,j}^r \quad \forall i \in [1, I_j^o] \quad (10)$$

However, the calculation for the second type of delay is more complex. According to each vehicle's arriving time at the stop bar ($T_{i,j}^r$), approaching vehicles can be divided into three groups (as shown in Figure 1):

Arrival 1. Those that arrive before the end of green time in cycle k ,

Arrival 2. Those that arrive after the end of green in cycle k but before the end of green in cycle $k+1$, and

Arrival 3. Those that arrive after the end of green in cycle $k+1$.

Two binary variables, $y_{i,j}^k$ and $y_{i,j}^{k+1}$, are introduced to determine vehicles from these three arrival types. The relationships between the binary variables and the vehicle's arriving time to the stop bar are expressed as Equations 11 through 14:

$$T_{i,j}^r > t_{j,k} + g_{j,k} - y_{i,j}^k M \quad (11)$$

$$T_{i,j}^r \leq t_{j,k} + g_{j,k} + (1 - y_{i,j}^k) M \quad (12)$$

$$T_{i,j}^r > t_{j,k+1} + g_{j,k+1} - y_{i,j}^{k+1} M \quad (13)$$

$$T_{i,j}^r \leq t_{j,k+1} + g_{j,k+1} + (1 - y_{i,j}^{k+1}) M \quad (14)$$

where

$T_{i,j}^r$ = projected arrival time of the i th vehicle of phase j at the stop bar,

$y_{i,j}^k, y_{i,j}^{k+1}$ = binary variables, and

M = large number constant.

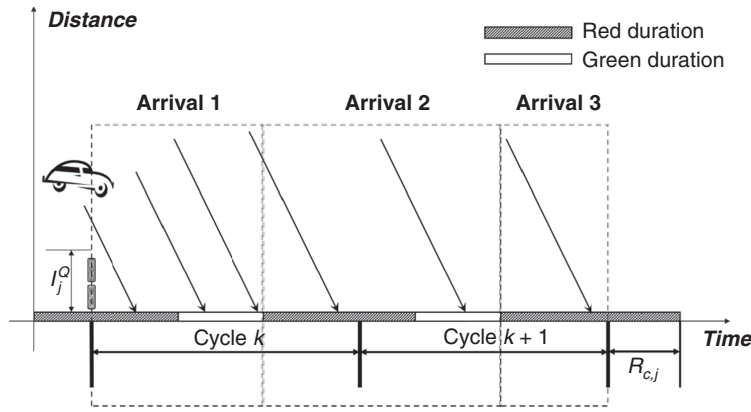


FIGURE 1 Three arrival types for vehicles arriving at intersection.

When $y_{i,j}^k$ equals 1, the i th vehicle of phase j will be projected to arrive at the stop bar before the end of green in cycle k . The meaning of $y_{i,j}^{k+1}$ is similar but applies for cycle $k + 1$. Any vehicle that arrives before the end of green in cycle k must arrive before the end of green in cycle $k + 1$, so $y_{i,j}^k \leq y_{i,j}^{k+1}$ always holds.

The pair of $(y_{i,j}^k, y_{i,j}^{k+1})$ values for a vehicle uniquely defines its arrival type: (1, 1) for Arrival 1, (0, 1) for Arrival 2, and (0, 0) for Arrival 3. Because the delay calculation varies between arrival types, the value of $(y_{i,j}^k, y_{i,j}^{k+1})$ is used to find the right delay calculations for each vehicle, as shown in Equations 15 through 20:

$$d_{i,j} \geq d_{i,j}^I - (1 - y_{i,j}^k)M - (1 - y_{i,j}^{k+1})M \quad (15)$$

$$d_{i,j} \leq d_{i,j}^I + (1 - y_{i,j}^k)M + (1 - y_{i,j}^{k+1})M \quad (16)$$

$$d_{i,j} \geq d_{i,j}^{II} - y_{i,j}^k M - (1 - y_{i,j}^{k+1})M \quad (17)$$

$$d_{i,j} \leq d_{i,j}^{II} + y_{i,j}^k M + (1 - y_{i,j}^{k+1})M \quad (18)$$

$$d_{i,j} \geq d_{i,j}^{III} - y_{i,j}^k M - y_{i,j}^{k+1} M \quad (19)$$

$$d_{i,j} \leq d_{i,j}^{III} + y_{i,j}^k M + y_{i,j}^{k+1} M \quad (20)$$

where $d_{i,j}^I$, $d_{i,j}^{II}$, $d_{i,j}^{III}$ refer to the estimated delay of vehicles from Arrival 1, 2, or 3, respectively.

Two other binary variables, $\theta_{i,j}^k$ and $\theta_{i,j}^{k+1}$ are introduced in the formulation and describe the vehicle's time when leaving the intersection. A vehicle is projected to clear the intersection before the end of green phase j in cycle k if its $\theta_{i,j}^k$ equals 1, and 0 if otherwise. The meaning of $\theta_{i,j}^{k+1}$ is similar to that of $\theta_{i,j}^k$, but for cycle $k + 1$. Combined, these four binary variables ($y_{i,j}^k, y_{i,j}^{k+1}, \theta_{i,j}^k, \theta_{i,j}^{k+1}$) in Constraints 21 and 22 indicate how Vehicle 1 arrives and leaves the intersection in relation to the two cycles in the planning horizon.

$$\theta_{i,j}^k \leq y_{i,j}^k \quad (21)$$

$$\theta_{i,j}^k + \theta_{i,j}^{k+1} \leq y_{i,j}^{k+1} \quad (22)$$

The two constraints enforce three rules. First, vehicles arriving after the end of green in cycle k cannot clear the intersection during

cycle k ; second, vehicles arriving after the end of green in cycle $k + 1$ cannot clear the intersection in the planning horizon; third, vehicles can never leave the intersection in both cycle k and $k + 1$. The case in which a vehicle does not clear the intersection is not prohibited by these constraints.

Formulations for Arrival 1

Delay occurs when the vehicle's arrival time is earlier than the start of the green. The queue ($q_{i,j}^I$) in number of vehicles arriving before the i th vehicle's arrival and the time ($t_{i,j}^I$) this vehicle joins the queue are the two important variables in its delay calculation. (The superscripts I, II, and III here and elsewhere indicate the arrival type.) Given an average length of vehicles (L_s), the arrival time of vehicle i at the back of the queue is calculated as follows:

$$t_{i,j}^{r,I} = T_{i,j}^r - \frac{q_{i,j}^I L_s}{v_j} \quad (23)$$

For the i th vehicle of phase j , $(i - 1)$ vehicles arrived before it. However, some of those vehicles may have left the intersection when the i th vehicle approached. Figure 2 shows three typical situations when the queue length ($q_{i,j}^I$) on the arrival of the i th vehicle is calculated.

The vehicle on the left arrives before the green of cycle k starts. Hence, $\lfloor (i - 1)/N_j \rfloor$ vehicles arrived before it and none left the intersection when it approached. However, the green had been on for $(t_{i,j}^r - t_{j,k})$ s when the middle vehicle approached the intersection. Some of the vehicles arrived before it left. Therefore, the queue at the vehicle's arrival at the stop bar reduces to $\lfloor (i - 1)/N_j \rfloor - s_j(t_{i,j}^r - t_{j,k})$. Vehicles arriving late enough may have $\lfloor (i - 1)/N_j \rfloor \leq s_j(t_{i,j}^r - t_{j,k})$, meaning all the vehicles arriving before it have cleared the intersection, and there would be no queues ahead of it by the time it arrives. This situation is illustrated by the vehicle on the right in Figure 2.

A binary variable ($\sigma_{i,j}^I$) is used in Equations 24 and 25 to distinguish whether a vehicle arrives before or after the start of green.

$$t_{i,j}^{r,I} \leq t_{j,k} + (1 - \sigma_{i,j}^I)M \quad (24)$$

$$t_{i,j}^{r,I} > t_{j,k} - \sigma_{i,j}^I M \quad (25)$$

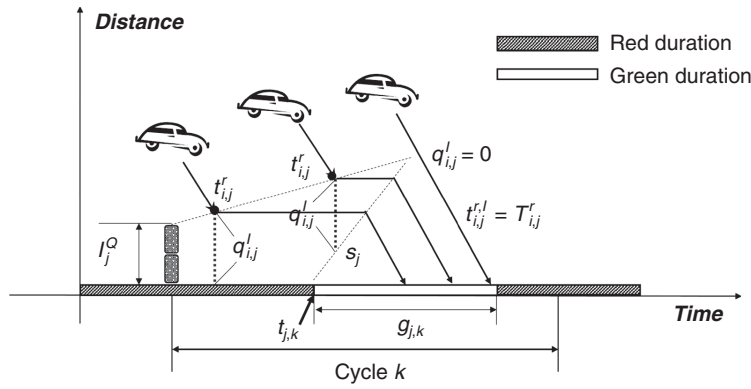


FIGURE 2 Three types of queues on arrival of i th vehicle.

Hence, the number of vehicles arriving before the arrival of the i th vehicle in the case of Arrival 1 can be calculated with the following equations, which correspond to the three types of queues illustrated in Figure 2:

$$q_{i,j}^l \geq \left\lfloor \frac{i-1}{N_j} \right\rfloor - (1 - \sigma_{i,j}^1)M \quad (26)$$

$$q_{i,j}^l \geq \left\lfloor \frac{i-1}{N_j} \right\rfloor - s_j(t_{i,j}^r - t_{j,k}^r) - \sigma_{i,j}^1M \quad (27)$$

$$q_{i,j}^l \geq 0 \quad (28)$$

After arriving at the intersection, the vehicle either clears the intersection in the current cycle k ($\theta_{i,j}^k = 1$) or waits for the green in the next cycle ($\theta_{i,j}^k = 0$). Only if the queues on a vehicle's arriving can be dissipated during the rest of green time would the vehicle be able to clear the intersection during the current cycle k . This scenario can be mathematically expressed:

$$\frac{q_{i,j}^l}{s_j} \leq g_{j,k} + (1 - \sigma_{i,j}^1)M + (1 - \theta_{i,j}^k)M \quad (29)$$

$$\frac{q_{i,j}^l}{s_j} > g_{j,k} - (1 - \sigma_{i,j}^1)M - \theta_{i,j}^kM \quad (30)$$

$$\frac{q_{i,j}^l}{s_j} + t_{i,j}^r \leq t_{j,k} + g_{j,k} + \sigma_{i,j}^1M + (1 - \theta_{i,j}^k)M \quad (31)$$

$$\frac{q_{i,j}^l}{s_j} + t_{i,j}^r > t_{j,k} + g_{j,k} - \sigma_{i,j}^1M - \theta_{i,j}^kM \quad (32)$$

A vehicle clears the intersection only if all the $(i - 1)$ vehicles have left. This waiting time is its delay. However, those that cannot clear the intersection in cycle k have to wait longer for the next green. This extra waiting time ($P_{i,j}^k$) equals the red duration between the two consecutive green lights, shown in Figure 3.

After all the above arrival and departure scenarios have been listed, the delay for each case can be formulated in the following inequalities:

$$d_{i,j}^l \geq \frac{q_{i,j}^l}{s_j} + t_{j,k} - t_{i,j}^r - (1 - \sigma_{i,j}^1)M - (1 - \theta_{i,j}^k)M \quad (33)$$

$$d_{i,j}^l \geq \frac{q_{i,j}^l}{s_j} + t_{j,k} - t_{i,j}^r + P_{i,j}^k - (1 - \sigma_{i,j}^1)M - \theta_{i,j}^kM \quad (34)$$

$$d_{i,j}^l \geq \frac{q_{i,j}^l}{s_j} - \sigma_{i,j}^1M - (1 - \theta_{i,j}^k)M \quad (35)$$

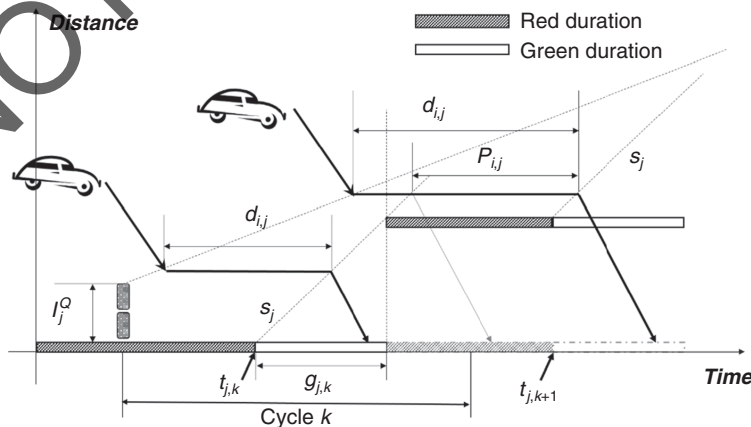


FIGURE 3 Two types of vehicle delay.

$$d_{i,j}^I \geq \frac{q_{i,j}^I}{s_j} + P_{i,j}^k - \sigma_{i,j}^I M - \theta_{i,j}^k M \quad (36)$$

$$P_{i,j}^k = t_{j,k+1} - (t_{j,k} + g_{j,k}) \quad (37)$$

Formulations for Arrival 2

The difference between Arrival 1 and Arrival 2 is small. The cycle superscript is $k + 1$ instead of k in most of the formulations. However, the number of vehicles that cleared the intersection during cycle k (V_j^k) should be taken into consideration when the index i is used to calculate the queues in Arrival 2. Changes to Inequalities 26 through 28 are made as follows:

$$q_{i,j}^{\text{II}} \geq \left| \frac{i-1-V_j^k}{N_j} \right| - (1-\sigma_{i,j}^{\text{II}})M \quad (38)$$

$$q_{i,j}^{\text{II}} \geq \left| \frac{i-1-V_j^k}{N_j} \right| - s_j (t_{i,j}^{\text{II}} - t_{j,k+1}) - \sigma_{i,j}^{\text{II}} M \quad (39)$$

$$q_{i,j}^{\text{II}} \geq 0 \quad (40)$$

$$V_j^k = \sum_{i=t_j^{\text{II}}+1}^{I_j} \theta_{i,j}^k \quad (41)$$

Similar to the extra wait time ($P_{i,j}^k$) in Arrival 1, vehicles that cannot clear the intersection in cycle $k + 1$ ($\theta_{i,j}^{k+1} = 0$) have longer delay with an extra waiting time ($P_{i,j}^{k+1}$) added. However, this wait time cannot be calculated definitively with the start times of the phase within the planning horizon because the start time of the phase in cycle $k + 2$ is out of the planning horizon. This extra wait time is estimated by introducing a red time compensation constant ($R_{c,j}$). As illustrated on the right of the time bar in Figure 1, the constant equals the total time duration from the beginning of a cycle to the beginning of the phase in the original signal timing plan. Hence the extra wait time can be calculated as in Equation 42:

$$P_{i,j}^{k+1} = t_{j,k+1} + v_{j,k+1} + R_{c,j} - (t_{j,k+1} + g_{j,k+1}) \quad (42)$$

Formulations for Arrival 3

In the Arrival 3 situation, vehicles arrive after the green of phase j in cycle $k + 1$ and will not clear the intersection within the planning horizon. The calculation of queues on vehicle i 's arrival should take into consideration the vehicles that have already departed the intersection during cycle $k + 1$ (V_j^{k+1}), which should be subtracted as in Equation 43. The delay is computed as in Equation 45.

$$q_{i,j}^{\text{III}} \geq \left| \frac{(i-1) - V_j^k - V_j^{k+1}}{N_j} \right| \quad (43)$$

$$V_j^{k+1} = \sum_{i=t_j^{\text{III}}+1}^{I_j} \theta_{i,j}^{k+1} \quad (44)$$

$$d_{i,j}^{\text{III}} \geq \frac{q_{i,j}^{\text{III}}}{s_j} + t_{j,k+1} + v_{j,k+1} + R_{c,j} - t_{i,j}^{\text{III}} \quad (45)$$

There are a few more constraints on the green durations in cycle k and $k + 1$. Inequalities 46 and 47 ensure that the green duration is long enough to allow no vehicle to wait more than one cycle. With these constraints, no one phase will become oversaturated while serving bus priority requests:

$$g_{j,k} \geq \frac{\left\lfloor \frac{I_j^{\text{O}}}{N_j} \right\rfloor}{s_j} \quad (46)$$

$$g_{j,k+1} \geq \frac{\left\lfloor \frac{(I_j^{\text{O}} + A_j - V_j^k)}{N_j} \right\rfloor}{s_j} \quad (47)$$

$$A_j = \sum_{i=t_j^{\text{O}}+1}^{I_j} y_{i,j}^k \quad (48)$$

where A_j is the total number of vehicles belonging to Arrival 1.

SIMULATION EVALUATION

Evaluation Platform

A traffic simulation was built to evaluate the performance of the PAPSCCI model. The simulation platform was adopted from the research of Zeng et al. (8). The platform consists of three main modules: optimization, signal control, and simulation. At the beginning of every cycle, the signal control module gathers information of all the vehicles that would be approaching the intersection during the following planning horizon. These pieces of information include vehicle speed, vehicle location, occupancy, and vehicle type, all of which can be obtained through CV technology in real time. All information is extracted from the simulation module and is supplied to the optimization module, where the PAPSCCI model is coded. Optimization is conducted with IBM CPLEX and follows the PAPSCCI model. The optimized signal timing data are then sent back to the simulation module to continue the traffic simulation. Simulation is conducted with PTV VISSIM.

Simulation Test Bed

The test intersection was designed as a typical four-leg intersection shown in Figure 4. Three bus lines were designed for different test scenarios. Route 202 travels eastbound, with a headway of 300 s and occupancy of 30 passengers. It requests Phase 2. Route 303 requests Phase 3 at this intersection, its headway is 360 s, and there are 35 passengers on each bus. Route 401 enters the intersection from Phase 4. The bus headway for the route is 400 s, and each bus carries 25 passengers. All buses travel at about 60 km/h (40 mph). Other vehicle types on the road are CV autos with onboard units and regular autos. Both types of vehicles travel at 60 km/h with an average of 1.5 passengers on board. Since the PAPSCCI model collects data from all the vehicles that would arrive at the intersection during a planning horizon (i.e., two cycles or 120 sec), the approach length of the eight movements is set to be slightly over 2000 m in the simulation test bed.

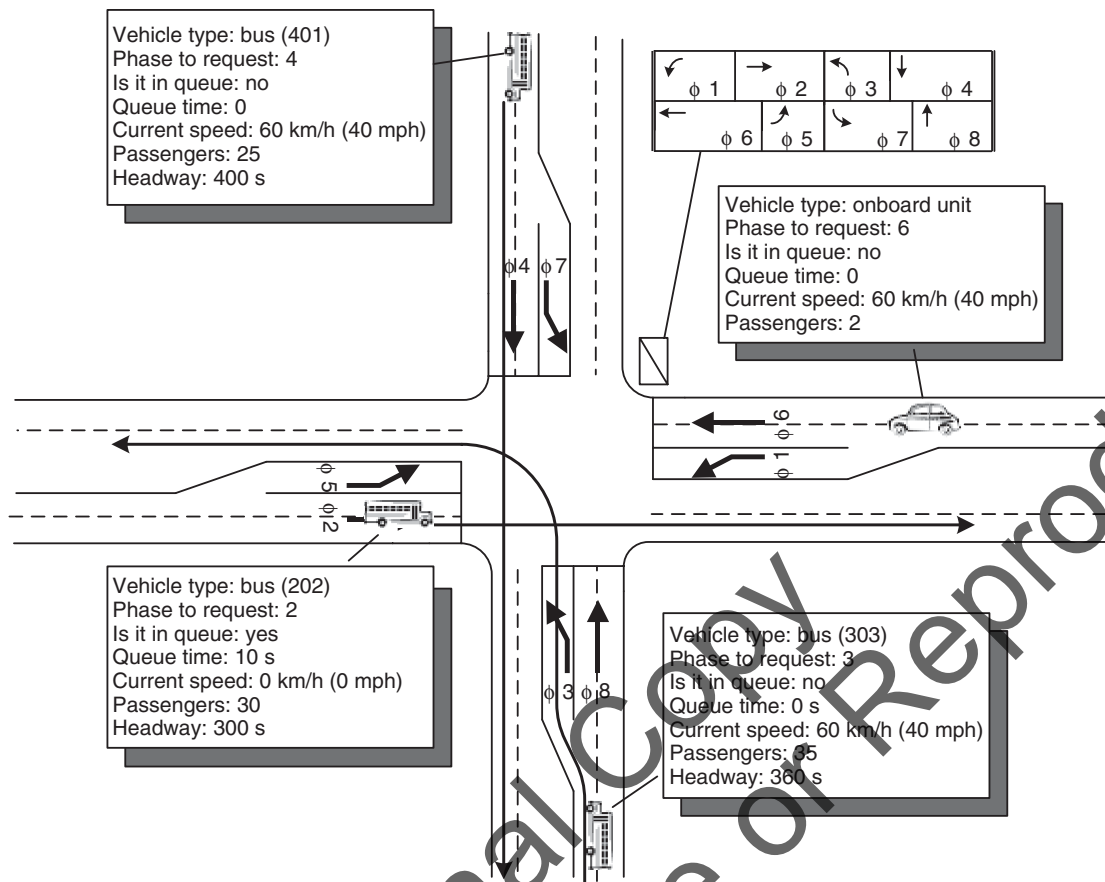


FIGURE 4 Intersection used in simulation study (B).

The phase sequence on this test intersection is shown in Figure 4. Other parameters for this test intersection, including number of lanes of each phase, traffic volumes, and background signal timing plans, are listed in Table 1. The phase splits and cycle length (60 s) are optimized in SYNCHRO, and this baseline timing serves as a background setup for the simulation and evaluation with the PAPSCCI model. For each test scenario, five random seeds are simulated. The delay results are the averages for the five runs.

RESULTS ANALYSIS

PAPSCCI for Autos Only

Autos-only is the basic test scenario for the PAPSCCI model evaluation. Simulations of SYNCHRO optimization and PAPSCCI optimization

are both conducted with no bus operations. SYNCHRO optimization refers to the simulation runs that use the fixed timing obtained from offline SYNCHRO optimizations, listed in Table 1.

The simulation results of vehicle and person delays are listed in Table 2, along with the delay changes in percentage between these two optimization types. Unlike the fixed signal timings from SYNCHRO, the PAPSCCI model allows the cycle length to change, which gives more flexibility to timing adjustment. It is apparent that the CV information allows the signal control to be more adaptive to cycle-by-cycle vehicle flow fluctuations, generating 10% delay savings.

PAPSCCI with TSP

The PAPSCCI with TSP test case was designed to evaluate the performance of the PAPSCCI model when multiple conflicting bus lines are in operation. Up to three bus lines are included.

TABLE 1 Background Setup for Test Intersection

	Phase							
	phi 1	phi 2	phi 3	phi 4	phi 5	phi 6	phi 7	phi 8
Number of lanes	1	2	1	2	1	2	1	2
Volume (vehicles)	112	616	90	381	78	784	101	280
Optimal splits	11	24	11	14	10	25	11	14

TABLE 2 Vehicle Delays and Person Delays for Auto-Only Scenario

Delay Type	SYNCHRO Optimization	PAPSCCI Optimization	Percentage Delay Change
Vehicle delay (s)	21.74	19.45	-10.57
Person delay (s)	21.64	19.20	-11.27

NOTE: Results consider 100% penetration rate of CV technology.

TABLE 3 Vehicle Delays and Person Delays for Single-Bus-Line Scenario

Delay Type	Vehicle Type	SYNCHRO Optimization	PAPSCCI Optimization	Percentage Delay Change	Percentage Delay Change Without Bus
Vehicle delay (s)	Auto	21.78	19.78	-9.18	na
	Bus	22.54	14.14	-37.27	na
	Total	21.78	19.72	-9.45	-10.57
Person delay (s)	Auto	21.74	19.38	-10.85	na
	Bus	22.54	13.64	-39.50	na
	Total	21.74	19.02	-12.67	-11.27

NOTE: Results consider 100% penetration rate of CV technology. na = not applicable.

For the case of a single bus line, Table 3 lists the delay changes of both vehicle delay and person delay for each vehicle type. In comparison, the PAPSCCI model can effectively decrease both vehicle delay and person delay for buses. A 37% greater delay reduction was observed for the buses. For auto delay, vehicle delay in Table 3 (i.e., 21.78 s) is almost the same as that in Table 1 (i.e., 21.74 s), because auto vehicle arrivals are exactly the same, except for the added bus line of Route 202. This added bus line decreased the vehicle delay improvement on total traffic by about 1.1%. However, for person delays, it was 1.4% better. These results show that the PAPSCCI model does favor vehicles with more passengers, such as buses, over vehicles with fewer passengers.

If a single bus line case is considered to be a scenario of light bus activity, then two and three bus line cases can be considered as medium and heavy bus activity scenarios, respectively. Figure 5 shows column charts for the delay changes after PAPSCCI optimization in scenarios of multiple bus lines. In the three scenarios, buses experienced 38%, 49%, and 28% delay decreases compared with autos, respectively. Another trend is that with the increase in bus activities, delay improvements of buses and autos first get better and then become worse. Although all three designed bus routes have conflicting routes, they have different headways, so they may not always show up in the same cycle competing for green times. When only two bus lines are running through the intersection, the times when buses of different routes are actually conflicting at the intersection are much fewer than the situation of having three bus lines in operation. This result indicates that a priority strategy at a single intersection is most effective when the conflicting bus activities are at a medium level.

Penetration Rate Evaluation

The PAPSCCI model is built on an ideal case in which all vehicles are equipped with CV devices; however, this case is not realistic in the foreseeable future. Therefore, the impacts of market penetration on the performance of the PAPSCCI model were evaluated. Five penetration rates—100%, 80%, 60%, 40%, and 20%—were evaluated for two scenarios: auto-only and auto with a single bus line.

So that each vehicle is properly indexed and its position in the queue estimated, necessary revisions to the formulation are made with the penetration rate factor. When the penetration rate is lower, more vehicles without CV devices would not be recognized and indexed by the system when approaching the intersection. This causes two problems with the model:

- First, it is inaccurate to use $(i - 1)$ as the number of vehicles that have arrived before vehicle i in the calculation of the queue position of the i th vehicle.
- Second, with fewer autos recognized by the system, the person delay of buses gains higher weights in the objective function.

To address the first problem, gross estimations must be made on the portion of vehicles that are not seen by the connected vehicle system. A known penetration rate (PenRate) and a random distribution of equipped vehicles are assumed, and then a naive estimation can be applied by dividing the penetration rate by the total number of vehicles actually seen and indexed by the system. Constraints 10, 26, 27, 38, 39, 43, 46, and 47 are revised into Constraints 49 through 56. To account for the second problem, the formulation was revised by dividing the person delay of autos by the penetration rate.

$$d_{i,j}^o \geq \frac{\left\lfloor \frac{i-1}{N_j} \right\rfloor}{(s_j \times \text{PenRate}) + t_{i,k} + t_{\text{stop},i,j}} \quad \forall i \in [1, I_j^o] \quad (49)$$

$$q_{i,j}^I \geq \frac{\left\lfloor \frac{i-1}{N_j} \right\rfloor}{\text{PenRate} - (1 - \sigma_{i,j}^I)M} \quad (50)$$

$$q_{i,j}^I \geq \frac{\left\lfloor \frac{i-1}{N_j} \right\rfloor}{\text{PenRate} - s_j(t_{i,j}^{r,I} - t_{j,k}) - \sigma_{i,j}^I M} \quad (51)$$

$$q_{i,j}^{II} \geq \frac{\left\lfloor \frac{i-1-V_j^k}{N_j} \right\rfloor}{\text{PenRate} - (1 - \sigma_{i,j}^{II})M} \quad (52)$$

$$q_{i,j}^{II} \geq \frac{\left\lfloor \frac{i-1-V_j^k}{N_j} \right\rfloor}{\text{PenRate} - s_j(t_{i,j}^{r,II} - t_{j,k+1}) - \sigma_{i,j}^{II} M} \quad (53)$$

$$q_{i,j}^{III} \geq \frac{\left\lfloor \frac{(i-1) - V_j^k - V_j^{k+1}}{N_j} \right\rfloor}{\text{PenRate}} \quad (54)$$

$$g_{i,k} \geq \frac{\left\lfloor \frac{I_j^o}{N_j} \right\rfloor}{(s_j \times \text{PenRate})} \quad (55)$$

$$g_{i,k+1} \geq \frac{\left\lfloor \frac{I_j^o + A_j - V_j^k}{N_j} \right\rfloor}{(s_j \times \text{PenRate})} \quad (56)$$

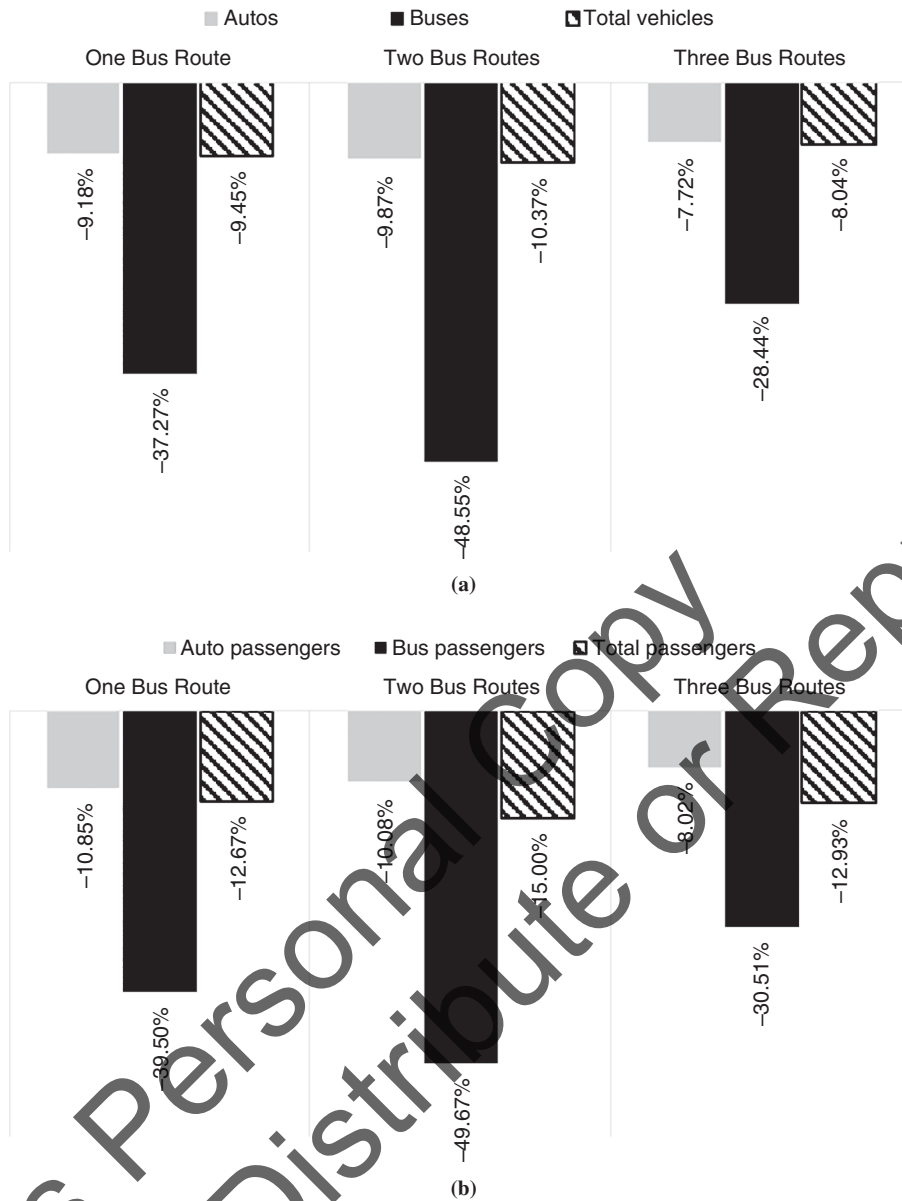


FIGURE 5 Delay changes with multiple bus lines: (a) vehicle delay change and (b) person delay change. Results assume 100% penetration rate of CV technology.

Figure 6 shows column charts for both vehicle and person delay changes after optimization with the PAPSCCI model in the scenario in which only one bus route, Route 202, is running. Figure 6, *a* and *b*, shows the general trend that the performance of the PAPSCCI model worsens with the decrease in the penetration rate. The worsening effects become sharper when the penetration rates drops below 40%. The results indicate that (a) the adjustment factor helps slow the worsening of model effectiveness and (b) the threshold for PAPSCCI to perform effectively with a single bus line is around 30%. This outcome is consistent with the conclusion made by Goodall that the minimum penetration rate for demonstrating benefits in any CV application is typically near 20% to 30% (16).

Autos are the most affected by the lower penetration rate of all vehicle types in the tests. When the penetration rate is lower than 60%, vehicle delay and person delay for autos are increased after

the PAPSCCI optimization. This increase is because their vehicle information cannot be collected by the CV system and therefore they are not counted in the optimization.

All buses are assumed to be equipped with CV devices, so their delay changes appear to benefit from the decrease of penetration rate at first but are then negatively affected when penetration rate continues to drop. A smaller penetration rate reduces the accuracy in estimating auto behaviors on the road and inevitably affects the decision on granting signal priority to buses.

To test further the influence of penetration rate on the performance of the PAPSCCI model, more penetration rate tests were made with multiple bus lines running through the intersection. Figure 7 compares changes in person delay for various bus route scenarios. Combining the results from Figures 7 and 6 shows that the threshold for the CV penetration rates for the PAPSCCI model to generate any benefit is about 30%.

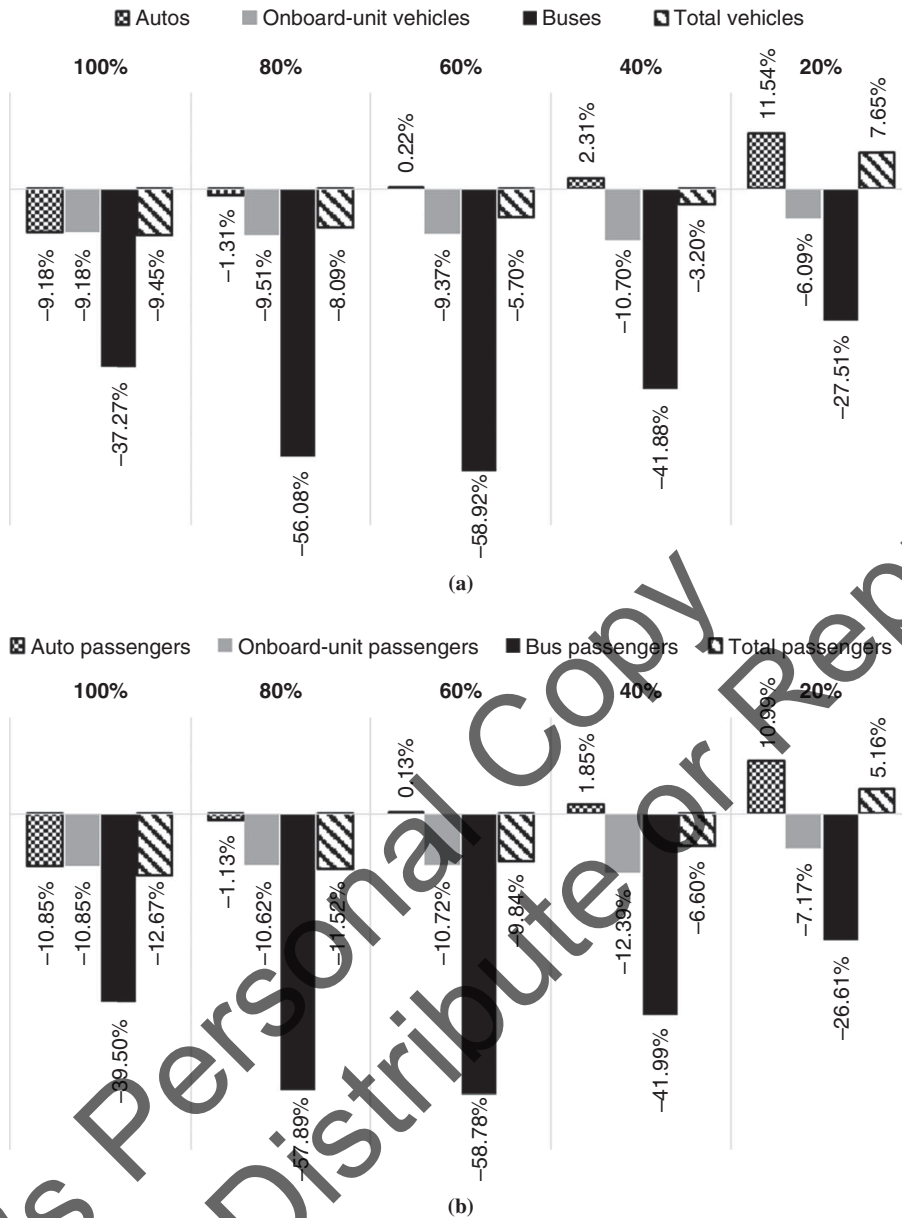


FIGURE 6 Delay changes with various penetration rates: (a) vehicle delay change and (b) person delay change.

CONCLUSION

A real-time signal control optimization model, PAPSCCI, was proposed. By using detailed CV information, the PAPSCCI model directly computes the person delay for every vehicle running through the intersection, instead of using conventional delay estimation models.

The evaluations with the PAPSCCI model were conducted on a simulation platform. Scenarios with multiple bus lines running through the test intersection were designed to test the model performance in an intersection with no, light, medium, and heavy bus activity. Test results showed that the PAPSCCI model can effectively decrease the person delay of buses in single and multiple conflicting bus line scenarios. As well, the PAPSCCI model can come up with good timing to reduce the intersection delay by around 10.5% when there are no bus lines running through the intersection, demonstrating the PAPSCCI model’s potential as an adaptive signal control system. Tests were also performed to evaluate the performance of the

PAPSCCI model with different penetration rates. Results show that although the delay changes after optimization become smaller with lower penetration rates, the PAPSCCI model can perform effectively with a 30% penetration rate.

However, this PAPSCCI model has some limitations. Because vehicle information is detected and recorded in the system before each optimization, and these data, including vehicle speed and route information, remain constant until the next optimization begins, the prediction accuracy in the model is affected. Also, the 2-km communication range of the CV technology at the intersection is too large for implementation. In future studies, a rolling optimization process may be used to minimize the negative impacts of prediction accuracy.

Calculation of the person delay for every vehicle in the planning horizon can be computationally intensive. A possible solution is to group vehicles together to reduce the number of binary variables. He et al. proposed an approach to optimizing signal timing that is based on vehicle platoons (17). Similarly, a person platoon instead

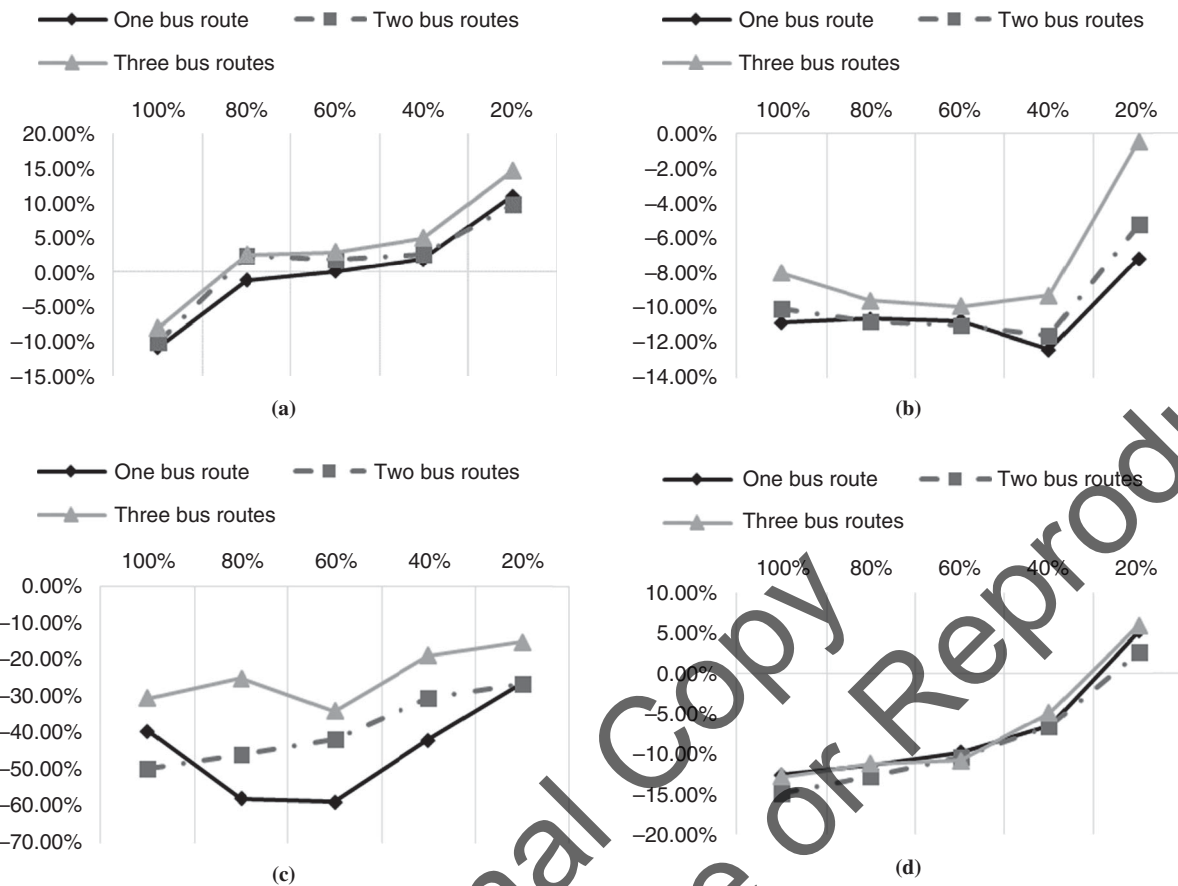


FIGURE 7 Person delay changes of penetration rate test with multiple bus lines: (a) auto, (b) onboard unit, (c) bus, and (d) total.

of a vehicle platoon can be used as an input in the optimization model to reduce the complexity of the PAPSCCI model. However, finding a likely person cluster based on less than 100% CV penetration rate is not a trivial task.

REFERENCES

1. *An Overview of Transit Signal Priority*. ITS America, Washington, D.C., 2004.
2. Vincent, R.A., B.R. Cooper, and K. Wood. *Bus-Actuated Signal Control at Isolated Intersections: Simulation Studies of Bus Priority*. TRRL Lab Report 814. Transportation and Road Research Laboratory, Crowthorne, United Kingdom, 1978.
3. Smith, H.R., B. Hemily, and M. Ivanovic. *Transit Signal Priority (TSP): A Planning and Implementation Handbook*. ITS America, Washington, D.C., 2005.
4. Janos, M., and P.G. Furth. Bus Priority with Highly Interruptible Traffic Signal Control: Simulation of San Juan's Avenida Ponce de Leon. In *Transportation Research Record: Journal of the Transportation Research Board, No. 1811*. Transportation Research Board of the National Academies, Washington, D.C., 2002, pp. 157–165.
5. Lee, J., and A. Shalaby. Rule-Based Transit Signal Priority Control Method Using a Real-Time Transit Travel Time Prediction Model. *Canadian Journal of Civil Engineering*, Vol. 40, No. 1, 2013, pp. 68–75.
6. Ma, W., Y. Liu, and X. Yang. A Dynamic Programming Approach for Optimal Signal Priority Control Upon Multiple High-Frequency Bus Requests. *Journal of Intelligent Transportation Systems*, Vol. 17, No. 4, 2012, pp. 282–293.
7. Li, M., Y. Yin, W.-B. Zhang, K. Zhou, and H. Nakamura. Modeling and Implementation of Adaptive Transit Signal Priority on Actuated Control Systems. *Computer-Aided Civil and Infrastructure Engineering*, Vol. 26, No. 4, 2011, pp. 270–284.
8. Zeng, X., Y. Zhang, K.N. Balke, and K. Yin. A Real-Time Transit Signal Priority Control Model Considering Stochastic Bus Arrival Time. *IEEE*

- Transactions on Intelligent Transportation Systems*, Vol. 15, No. 4, 2014, pp. 1657–1666.
9. He, Q., K.L. Head, and J. Ding. PAMSCOD: Platoon-Based Arterial Multi-Modal Signal Control with Online Data. *Transportation Research*, Vol. 20, No. 1, 2012, pp. 164–184.
10. Christofa, E., I. Papamichail, and A. Skabardonis. Person-Based Traffic Responsive Signal Control Optimization. *IEEE Transactions on Intelligent Transportation Systems*, Vol. 14, No. 3, 2013, pp. 1278–1289.
11. Christofa, E., K. Aboudolas, and A. Skabardonis. Arterial Traffic Signal Optimization: A Person-Based Approach. Presented at 92nd Annual Meeting of the Transportation Research Board, Washington, D.C., 2013.
12. Zeng, X., K.N. Balke, and P. Songchitruksa. *Potential Connected Vehicle Applications to Enhance Mobility, Safety, and Environmental Security*. Southwest Region University Transportation Center, Texas A&M Transportation Institute, Texas A&M University System, College Station, 2012.
13. Park, B.B., and J. Hu. *Transit Signal Priority with Connected Vehicle Technology*. UVA-2012-04. University of Virginia, Charlottesville, 2014.
14. Priemer, C., and B. Friedrich. A Decentralized Adaptive Traffic Signal Control Using V2I Communication Data. *Proc., 12th International IEEE Conference on Intelligent Transportation Systems*, 2009, pp. 1–6.
15. Head, L., D. Gettman, and Z. Wei. Decision Model for Priority Control of Traffic Signals. In *Transportation Research Record: Journal of the Transportation Research Board, No. 1978*. Transportation Research Board of the National Academies, Washington, D.C., 2006, pp. 169–177.
16. Goodall, N.J. *Real-Time Prediction of Vehicle Locations in a Connected Vehicle Environment*. FHWA/VCTIR 14-R4. Virginia Center for Transportation Innovation Research, Charlottesville, 2013.
17. He, Q., K.L. Head, and J. Ding. Heuristic Algorithm for Priority Traffic Signal Control. In *Transportation Research Record: Journal of the Transportation Research Board, No. 2259*. Transportation Research Board of the National Academies, Washington, D.C., 2011, pp. 1–7.